

University of Groningen

Dictyostelium chemotaxis

Kortholt, Arjan; Kataria, Rama; Keizer-Gunnink, Ineke; Van Egmond, Wouter N.; Khanna, Ankita; Van Haastert, Peter J. M.

Published in:
Embo Reports

DOI:
[10.1038/embor.2011.210](https://doi.org/10.1038/embor.2011.210)

IMPORTANT NOTE: You are advised to consult the publisher's version (publisher's PDF) if you wish to cite from it. Please check the document version below.

Document Version
Publisher's PDF, also known as Version of record

Publication date:
2011

[Link to publication in University of Groningen/UMCG research database](#)

Citation for published version (APA):

Kortholt, A., Kataria, R., Keizer-Gunnink, I., Van Egmond, W. N., Khanna, A., & Van Haastert, P. J. M. (2011). Dictyostelium chemotaxis: essential Ras activation and accessory signalling pathways for amplification. *Embo Reports*, 12(12), 1273-1279. <https://doi.org/10.1038/embor.2011.210>

Copyright

Other than for strictly personal use, it is not permitted to download or to forward/distribute the text or part of it without the consent of the author(s) and/or copyright holder(s), unless the work is under an open content license (like Creative Commons).

The publication may also be distributed here under the terms of Article 25fa of the Dutch Copyright Act, indicated by the "Taverne" license. More information can be found on the University of Groningen website: <https://www.rug.nl/library/open-access/self-archiving-pure/taverne-amendment>.

Take-down policy

If you believe that this document breaches copyright please contact us providing details, and we will remove access to the work immediately and investigate your claim.

Downloaded from the University of Groningen/UMCG research database (Pure): <http://www.rug.nl/research/portal>. For technical reasons the number of authors shown on this cover page is limited to 10 maximum.

SUPPLEMENTARY INFORMATION

TableS1. Strains and conditions used in chemotaxis experiment. All indicated strains were tested for chemotaxis with the small population assay, and cells showing poor chemotaxis were also tested with the micropipette assay (experiment number 1, 5, 36, 38, 39 and 40, and *gβ*-null, *rasC*, *rasG*, and *rasC/G*-null cells). The single letter code refers to the experiments presented in Table I of the manuscript. Chemotaxis was measured in the absence or presence of 2 μM BPB (inhibition of PLA2), 20 μM LY (inhibition of PI3K) or 90 μM LY (inhibition of PI3K and TorC2).

Figure S1. Chemotaxis and RBD-Raf-GFP response of Ras mutants. A, Chemotaxis was tested to cAMP gradients with different steepness of the gradient (as shown in Fig 2C). The spatial gradient that induces half-maximal chemotaxis is defined as $(dC/dx)_{50}$. Cells lacking *rasC* or *rasG* exhibit good directional movement, whereas cells lacking both *rasC* and *rasG* do not exhibit significant chemotaxis ($CI < 0.1$) at the steepest gradient measured (100 nM/μm). Panel B shows representative images of RBD-Raf-GFP localization in *rasC/G*-null cells in buffer and at 4-6 s after addition of uniform cAMP, revealing no detectable cAMP-mediated translocation of RBD-Raf-GFP to the membrane of *rasC/G* null-cells

Figure S2. Translocation of LimEΔcoil-GFP from the cytoplasm to the cell boundary. LimEΔcoil-GFP binds to F-actin. Panels A show representative images of GFP-tagged cells in buffer, 4-6 s after addition of uniform cAMP, or in a cAMP gradient; the bar is 5 μm. Panel B shows the time course of translocation after uniform stimulation with 1 μM cAMP as means and SD of 8 cells; Panels C presents the response at 4-6 s after addition

of uniform cAMP with different concentrations; shown are means and SD of at least 8 cells.

Movie 1 and 2. Chemotaxis of wild-type and *sgc/pla2*-null/LY cells, respectively, both expressing RBD-Raf-GFP. A pipette containing 1 μ M cAMP is applied in a field of cells as indicated by the asterisks. Images were recorded with a confocal microscope at a frame rate of 8 frames/minute. The movie shows a brief transient translocation of RBD-Raf-GFP to the entire cell boundary in the first frame after application of the pipette, which is followed by the persistent accumulation of RBD-Raf-GFP at the leading edge. Both cell lines exhibit good directional movement towards the pipette in these steep cAMP gradients.

Movie 3. Ras response of *sgc/pla2*-null/LY cells in the presence of Latrunclin A. Images were recorded as described in the legend to Movie 1 and 2. The movie shows a translocation of RBD-Raf-GFP similar to that of wild-type cells.

Table S1. Strains and conditions used in chemotaxis experiment

exp #	Code	Cell line and inhibitors	pathways inhibited	pathways active
1	V	WT	-	PI3K + TorC2 + PLA2 + sGC
2	U	WT + 20 LY	PI3K	TorC2 + PLA2 + sGC
3	O	WT + 90 LY	PI3K + TorC2	PLA2 + sGC
4	T	WT + BPB	PLA2	PI3K + TorC2 + sGC
5	L	WT + 20 LY + BPB	PI3K + PLA2	TorC2 + sGC
6	U	<i>pi3k</i> -null	PI3K	TorC2 + PLA2 + sGC
7	L	<i>pi3k</i> -null + BPB	PI3K + PLA2	TorC2 + sGC
8	T	<i>pla2</i> -null	PLA2	PI3K + TorC2 + sGC
9	l	<i>pla2</i> -null + 20 LY	PI3K + PLA2	TorC2 + sGC
10	e	<i>pla2</i> -null + 90 LY	PI3K + PLA2 + TorC2	sGC
11	u	<i>pkbA</i> -null	PI3K	TorC2 + PLA2 + sGC
12	l	<i>pkbA</i> -null + BPB	PI3K + PLA2	TorC2 + sGC
13	s	<i>pia</i> -null	TorC2	PI3K + PLA2 + sGC
14	o	<i>pia</i> -null + 90 LY	TorC2 + PI3K	PLA2 + sGC
15	j	<i>pia</i> -null + BPB	TorC2 + PLA2	PI3K + sGC
16	e	<i>pia</i> -null + 20 LY + BPB	TorC2 + PI3K + PLA2	sGC
17	s	<i>pkbR1</i> -null	TorC2	PI3K + PLA2 + sGC
18	o	<i>pkbR1</i> -null + 90 LY	TorC2 + PI3K	PLA2 + sGC
19	j	<i>pkbR1</i> -null + BPB	TorC2 + PLA2	PI3K + sGC
20	e	<i>pkbR1</i> -null + 20 LY + BPB	TorC2 + PI3K + PLA2	sGC
21	r	<i>gc</i> -null	sGC	PI3K + TorC2 + PLA2
22	k	<i>gc</i> -null + 20 LY	sGC + PI3K	TorC2 + PLA2
23	d	<i>gc</i> -null + 90 LY	sGC + PI3K + TorC2	PLA2
24	h	<i>gc</i> -null + BPB	sGC + PLA2	PI3K + TorC2
25	c	<i>gc</i> -null + 20 LY + BPB	sGC + PI3K + PLA2	TorC2
26	a	<i>gc</i> -null + 90 LY + BPB	PI3K + TorC2 + PLA2 + sGC	-
27	m	<i>gc</i> -null/sGCΔCat + 20 LY + BPB	PI3K + PLA2 + cGMP	sGCp + TorC2
28	n	<i>gc</i> -null/sGCΔN + 20 LY + BPB	PI3K + PLA2 + sGCp	cGMP + TorC2
29	f	<i>gc</i> -null/sGCΔCat + 90 LY + BPB	PI3K + TorC2 + PLA2 + cGMP	sGCp
30	g	<i>gc</i> -null/sGCΔN + 90 LY + BPB	PI3K + TorC2 + PLA2 + sGCp	cGMP
31	p	<i>gc</i> -null/sGCΔCat + 90 LY	PI3K + TorC2 + cGMP	sGCp + PLA2
32	q	<i>gc</i> -null/sGCΔN + 90 LY	PI3K + TorC2 + sGCp	cGMP + PLA2
33	l	<i>pi3k/pla2</i> -null	PI3K + PLA2	TorC2 + sGC
34	o	<i>pkbA/pkbR1</i> -null	PI3K + TorC2	PLA2 + sGC
35	e	<i>pkbA/pkbR1</i> -null + BPB	PI3K + TorC2 + PLA2	sGC
36	h	<i>sgc/pla2</i> -null	sGC + PLA2	PI3K + TorC2
37	c	<i>sgc/pla2</i> -null + 20 LY	sGC + PLA2 + PI3K	TorC2
38	a	<i>sgc/pla2</i> -null + 90 LY	PI3K + TorC2 + PLA2 + sGC	-
39	b	<i>sgc/pla2/pkbR1</i> -null	TorC2 + PLA2 + sGC	PI3K
40	a	<i>sgc/pla2/pkbR1</i> -null + 90 LY	PI3K + TorC2 + PLA2 + sGC	-

Figure S1

A

Strain	(dC/dx) ₅₀ pM/μm
Wild-type	22 ± 2
<i>rasC/G</i> -null	> 900000
<i>rasC</i> -null	42 ± 5
<i>rasG</i> -null	88 ± 8

B

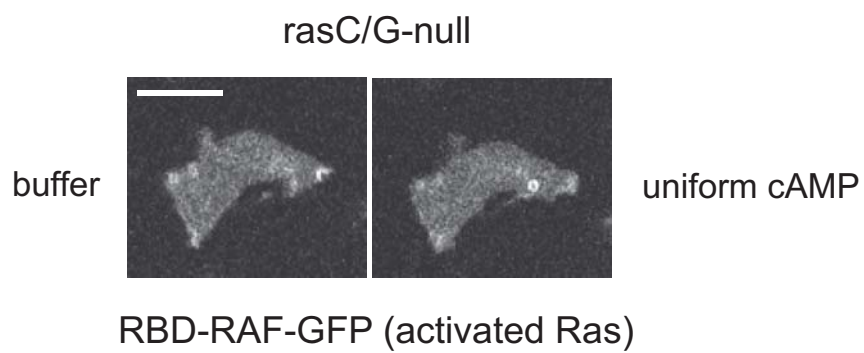


Figure S2

